



Update status EARTH July 2016

version 29 June 2016

**R.J. de Meijer, A. Zondervan, R. Lindsay, J. Stegenga, M.W. van Rooy,
S.W. Steyn, J. Whichello and W. van Westrenen**

Stichting Earth Antineutrino Tomography (EARTH)
de Weehorst
9321 XS Peize, The Netherlands
www.geoneutrino.nl



Preface

In this report you will find an account of the scientific and technological progress of our research in both Geoscience and Detector development. In my preface I will concentrate on the antineutrino detector development that brings us close to introducing to the world market applications for both routine safeguards and non-proliferation. On the one hand I am glad, honoured by and proud of the level that we have achieved but on the other hand the continuation and extension of this work brings us to a challenging (financial and) scientific phase. Therefore this time I choose to give our readers a preface and invite them to support us in reaching our goals.

As you will read both routine safeguards and non-proliferation applications are based on extrapolations from the present scientific results (such as ON/OFF status, its relative operational level and changes in the burn-up ratio of U and Pu), and the assumption that the basic mechanisms of the physics behind the effects are fully understood. At the appropriate time, and with sufficient funding, each will require a full assessment and successful demonstration as a practical and effective tool in support of its intended function.

This creates the situation that it will strategically and practically important if not of the highest priority, building a bridge between the involved Universities in South Africa, Scientific Institutions in The Netherlands and to be involved Universities in the United States of America and/or Canada.

In South Africa we found Universities gladly willing to establish a research chair together with such private party for a period of 5 years and support such chair with all the needed facilities needed to execute the remaining part of the program. Facilities are to be understood like, offices, laboratories, use of available equipment, staff for administrative and scientific guidance of the program and early as well as PhD students for the scientific work to be done. Potentially we have found a suitable candidate available who will be gladly prepared to fulfil the Chair

To open up such funding possibilities this status report may also be applied for judgement and decision making steps by those parties who are prepared and in principle willing to fund the remaining scientific part of our work in close cooperation with our partners in EARTH.

We will be glad and whole heartedly prepared to take responsibility for bringing parties together for investigating whether and how this financing could be materialised. For more information on this report or participation, please contact our director, Prof. dr. R.J. de Meijer (demeijer@geoneutrino.nl).

H.A. Koopmans
Acting Chairman and Treasurer Board EARTH



1. Introduction.

This report presents the progress of the EARTH programme since the last report, published in November 2014. An earlier report, EARTH PRP-007, published in July 2009 gave a comprehensive overview of the project and the reader is referred to EARTH PRP-007 for further details and background information.

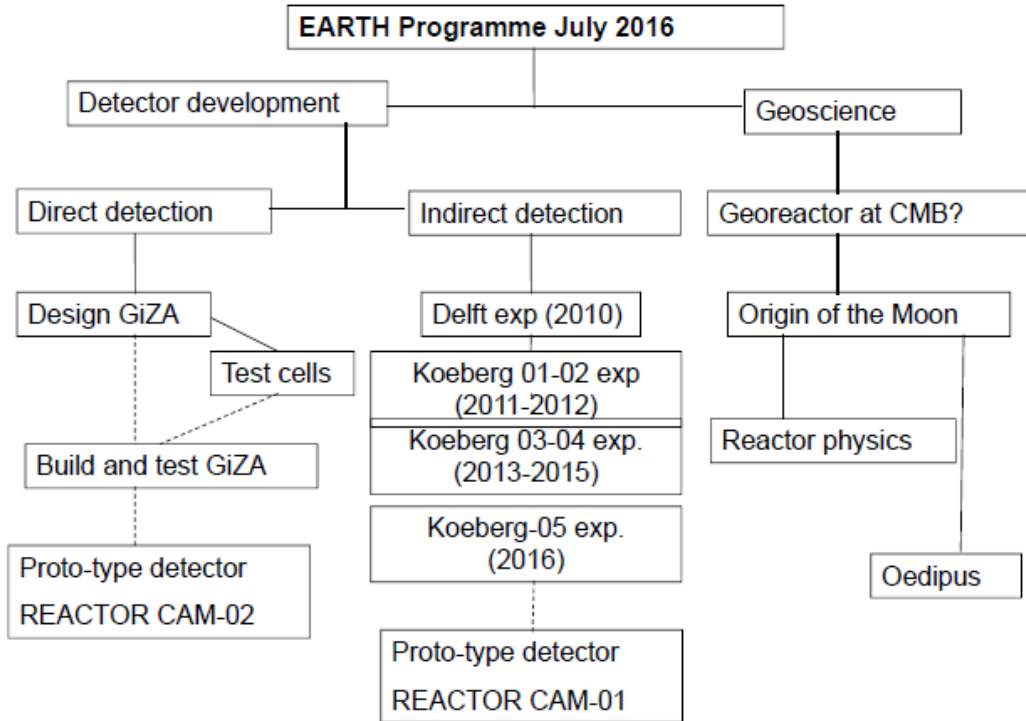


Figure 1. Schematic overview of various activities within the EARTH programme as at July 2016. The solid connecting lines indicate past and ongoing activities while the dashed lines are projections into the future.

The present and planned activities within the EARTH programme have schematically been presented in Figure 1. The solid lines indicate the parts of the programme, being either completed or in progress. The programme has two main activities: Antineutrino detector development and Geoscience aspects that could result from the eventual data collection of antineutrinos emitted by various radiogenic processes in Earth. The present update will be structured according to this scheme.

2. Detector development.

As indicated in Figure 1, detector development is one of the two main lines of research and development in the EARTH programme. A major goal of this research is the successful development of a compact antineutrino detector, offering a beneficial new tool to further strengthen the implementation of safeguards at nuclear reactor facilities,

globally. Achieving a compact detection system will also provide a significant tool for on-going efforts to detect undeclared activities associated with nuclear proliferation and clandestine nuclear weapons manufacture.

The preferred detection mechanism for antineutrinos depends on its energy. For energies above approximately 10 MeV Cherenkov radiation provides a direct way of antineutrino detection in which energy and incoming direction can be deduced. For low-energy ($< \sim 10$ MeV) antineutrinos Cherenkov radiation is not sensitive enough anymore and the most common detection is the so-called inverse beta-decay reaction in which the antineutrino is captured on a free proton and subsequently a positron and a neutron are emitted.

Initially we developed a compact detector named GiZA (see Figure 1) but the development was shelved because of our activities on the indirect detection.

The event is detected via the annihilation of the positron in which it combines with an electron and subsequently two annihilation quanta, each with an energy of $E=511\text{keV}$, are emitted. The neutron is detected after it has been captured by a nucleus. Commonly the capturing nucleus is H in liquid scintillators or plastic often doped with Gd (Gadolinium). In both the annihilation and the capture on H and Gd γ -radiation is emitted.

2.1 Indirect detection of antineutrinos.

2.1.1 Koeberg-03 measurements

In the previous progress report (EARTH PRP-10) we presented an overview of the measurements at Delft (*de Meijer et al., 2011*) and at the Koeberg nuclear power station (Koeberg-01 and Koeberg-02). Both measurements at Koeberg were plagued by instrumental problems, making the outcome of the measurements unreliable, hence a third series of measurements was conducted at the seismic vault direct under unit#1 of Koeberg. The EARTH PRP-11 progress report presents the description and initial analysis. The text and figures of EARTH PRP-11 were to a large extent taken from a manuscript placed on ArXiv (*de Meijer and Steyn, 2014*). In this document we report on the progress since November 2014.

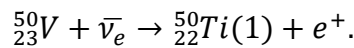
2.1.2 Koeberg-04 measurements

After a breakdown of part of the VENUS electronics, we replaced the VENUS+INTERWINNER hard- and software. By SCINTISPEC-MCA hardware and associated software, available at the Physics Department of the University of the Western Cape. After a couple of tests the following measurements were carried out:

- 23 December 2014 - 1 February 2015: Reactor=ON; ^{60}Co source in well counter;
- 2 February - 26 February 2015: Reactor in transition; ^{60}Co source in well counter;
- 27 February - 4 May 2015: Reactor=OFF; ^{60}Co source in well counter;
- 5 May – 31 May 2015: Reactor=OFF; Background measurement well counter;
- 21 August - 17 October 2015: Reactor=ON; Vanadium rod in well counter;
- 18 November – 2 December 2015: Reactor=ON; Background measurement.

The ^{60}Co measurements are intended to check whether a Reactor=ON/OFF effect is present. In case of an instrumental cause of the ON/OFF effect for ^{22}Na , a similar effect in magnitude is to be expected for the measurements with ^{60}Co . If the ^{22}Na effect is due to antineutrino interaction with ^{22}Na - β^+ -decay, no effect is expected for the β^- -decay of ^{60}Co , for which the β^+ -decay is energetically forbidden.

Figure 2 presents a schematic decay scheme of ^{50}V to ^{50}Ti . In fact ^{50}V decays in addition to the presented scheme by β^- -decay to the first excited state of ^{50}Cr at $E_x=783$ keV with $J^\pi=2^+$. The ratio between the EC and β^- -branch is 83:17 (*Table of Isotopes*). As follows from figure 2 the decay of ^{50}V to $^{50}\text{Ti}(1)$ is purely EC since $Q(\beta^+)=-368$ keV. However the antineutrino spectrum from the reactor provides antineutrinos ($\bar{\nu}_e$) with energies that may populate the $^{50}\text{Ti}(1)$ state through the reaction:



This reaction, if detected with a vanadium rod inside a well counter, could be detected with coincidence summing provided the cross section for this reaction allows it to be detected above room background. This reaction is similar to the reaction on ^{22}Na , but in the ^{50}V case the transition has a negative Q-value and is four times forbidden. On the other hand with the natural abundance of 0.25% and a half-life of $1.4 \cdot 10^{17}$ year, enhances the number of “target” nuclei per Bq by about 14 orders of magnitude.

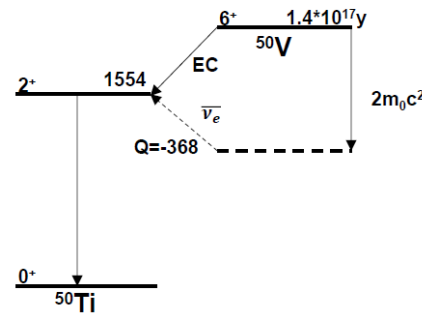


Figure 2. Schematic decay scheme of ^{50}V to ^{50}Ti .

The mass of our vanadium rod is 27.6 g and contains 0.069 g ^{50}V corresponding to $8.3 \cdot 10^{20}$ nuclei. The activity of the rod is about 0.13mBq. Assuming a cross section of $1.8 \cdot 10^{-25} \text{cm}^2$ (see section 2.1.4) and an antineutrino flux of $1.48 \cdot 10^{13} \text{cm}^{-2}\text{s}^{-1}$ the production rate would be about $2.2 \cdot 10^9$ $^{50}\text{Ti}(1)$ nuclei per second. With an almost 4π geometry this would correspond to a count rate of about $8 \cdot 10^{12}$ cph. The question is if the actual cross section for antineutrinos with $E>368$ keV is large enough to overcome the reduction due to the high degree of forbiddingness.

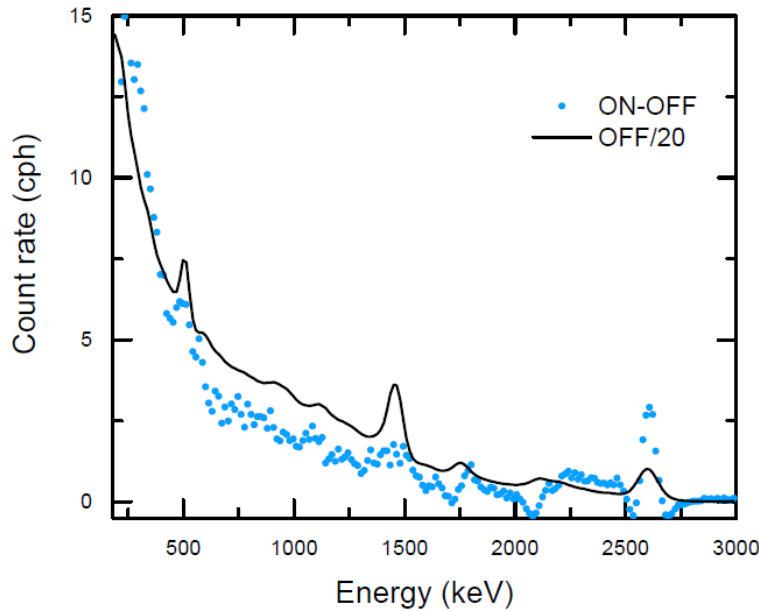


Figure 3. ON-OFF difference and scaled OFF background spectra of the well counter.

2.1.3 Analysis Koeberg-04 data.

Background measurements.

The Koeberg (KB) data set allows us to check and if needed correct our assumption in the analysis of the KB-03 data that background is not depending on reactor status. This assumption had to be made due to the absence of background measurements at Reactor=OFF. In the analysis of the KB-04 data special care was

taken on the energy matching of the spectra before determining their difference and their ratio for a number of RoI.

Figure 3 presents the ON-OFF background difference spectrum and the scaled OFF background spectrum. Whereas the OFF-spectrum clearly shows peaks at $E=511, 1460$ and 2614 keV due to natural radioactivity of the surrounding concrete, only the 2614 keV peak clearly shows up in the ON-OFF spectrum. This is consistent with excitation of the first excited state in ^{208}Pb by fast neutrons that have been able to cross the 8m concrete shielding between the reactor core and the detector set-up.

^{60}Co measurements.

A set of measurements with a $3\text{kBq } ^{60}\text{Co}$ source in the well counter were carried out in the period 23 December 2014-5 May 2015. The reactor was ON from 23 December to 31 January, in transition between 1 and 26 February and OFF from 27 February to 5 May. The source contains a small contamination of ^{58}Co affecting the spectrum below about 2 MeV.

The goal of this measurement is to clarify the issue on the nature of the reactor-status effect observed for ^{22}Na . If the effect is instrumental an equal effect is expected to show up with comparable size for ^{60}Co ; if the effect is related to antineutrinos affecting β^+ -decay the effect should not show up for ^{60}Co (β^- -decay).

To make the comparison between the measurements with both nuclei as close as possible, the analysis is restricted to the energy range of $2376\text{-}2719$ keV, being only populated by coincidence summing. In this energy range no contribution of ^{58}Co is expected. This was checked by measuring the decay rate for this RoI.

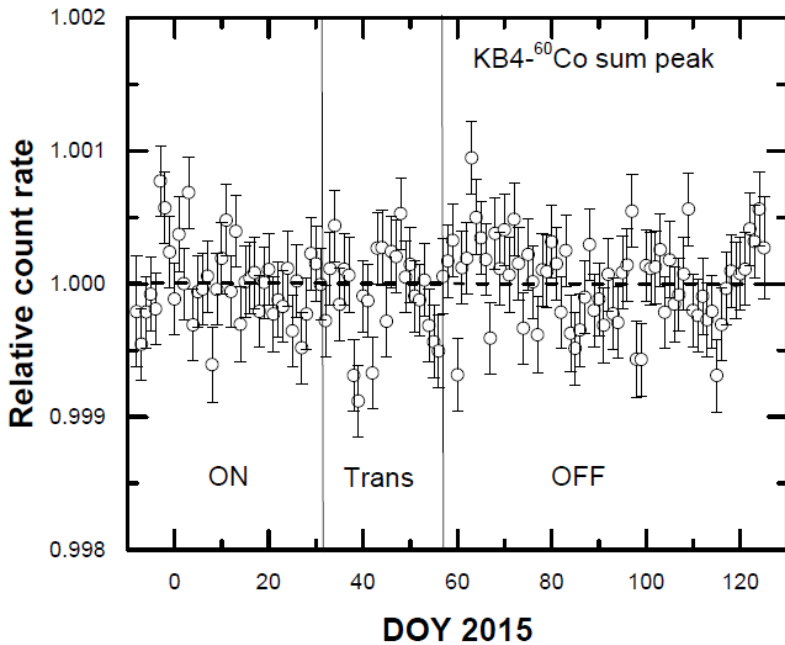


Figure 4. Normalised count rate for the ROI of 2376-2719 keV, encompassing the 1173 and 1333 keV sum peak in the decay of ^{60}Co .

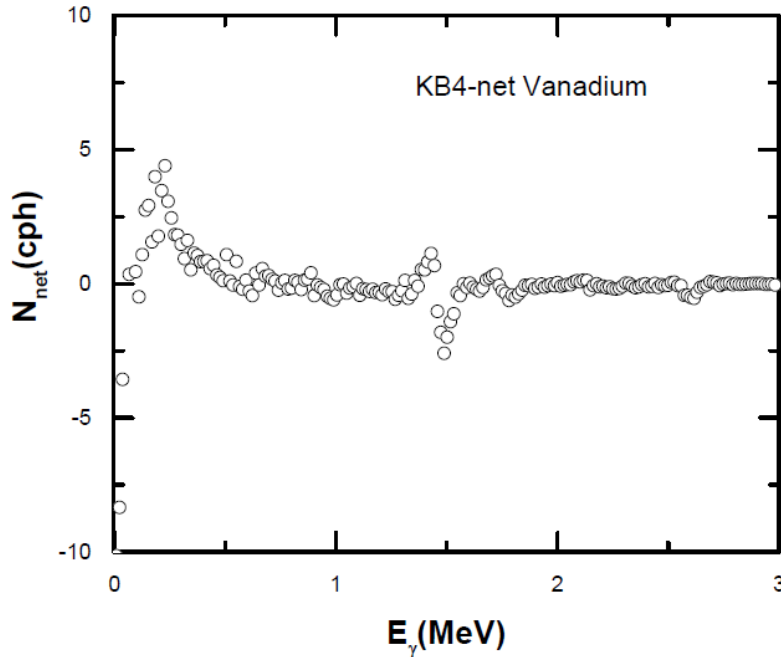


Figure 5. Net Vanadium spectrum.

As can be noticed from figure 4 no obvious difference is seen between the count rates during Reactor=ON and =OFF. From the weighted averages, including external uncertainties if the reduced χ^2 -values demand, a (ON-OFF)/OFF ratio of $(-0.2 \pm 0.6) \times 10^{-4}$ was obtained. This value is consistent with zero and is numerically an order of magnitude smaller than for the ROI-HI in ^{22}Na (see section 2.1.4).

^{50}V measurements.

Figure 5 presents the net spectrum obtained by subtracting a background spectrum from the spectrum obtained with a Vanadium-rod placed inside the well counter. During both measurements the reactor is ON. The measuring time for the V-spectrum is 58 days or 1392 h.

In the spectrum one sees the structures related to lines in the natural background spectrum being slightly

shifted and broadened. The net content of this spectrum is -95 cph compared to $7 \cdot 10^4$ cph in the V-spectrum. The value of -95 cph most likely reflects a slightly increased absorption of the room background spectrum due to the high density of the V-rod. The spectrum shows no evidence for a measurable effect of antineutrino capture on ^{50}V . This implies that either the assumed cross section (the one obtained for ^{22}Na ; see section 2.14) is not correct and/or the transition is hindered by more than 11 orders of magnitude.

2.1.4 Re-analysis of the Koeberg-03 data.

In the previous progress report and in the *de Meijer and Steyn (2014)* manuscript the analysis of the ^{22}Na +BG data was carried out under the assumption that there was no difference between the BG during Reactor=ON and =OFF. This assumption had to be made since we were unable to measure the BG during Reactor=OFF. The ON and OFF periods are summarised in Table 1. In KG-04 the BG was measured during both Reactor=ON and OFF and found to higher during the ON status by about 3% and slightly energy depended. Moreover in the earlier KB3 data analysis it was found that the on-line spectrum stabilisation was not sufficient.

Table 1. Reactor status dates for two measurement series with a ^{22}Na source.

Measurement series	Reactor status	Period (DOY 2013)	Dates
1	ON1	53-73	22 February-14 March 2013
	OFF1	85-112	26 March-22 April 2013
	ON2	117-140	27 April-20 May 2013
2	ON3	283-314	10 October-10 November 2013
	OFF2	320-361	16 November-27 December 2013
	ON4	367-405	2 January-9 February 2014

These two insights have led to a re-analysis of the data. Three regions of interest (RoI) were defined: TOT (170-2452 keV), MED (1151-1351 keV) and HI (1354-2452 keV). In this re-analysis besides the BG adjustments, the off-line spectrum stabilisation and re-calibration the data for each measurement sequence (ON-OFF-ON) were subjected to a regression analysis of the combined data sets for the three RoI. The analysis comprises three functions: a two parameter exponential dip function, being an instrumental effect, determined from the TOT data, and for each RoI a two-parameter linear function and a reactor-status function. So in total the analysis of the three combined RoI contains 13 parameters.



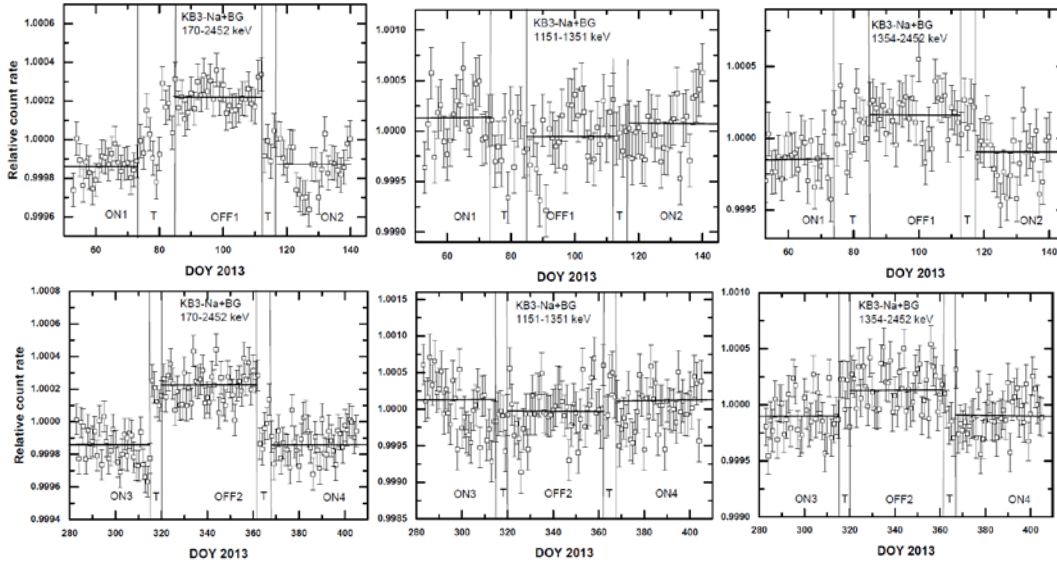


Figure 6. Daily averaged count rates in three RoI during the measurements in the periods February-May 2013 and Oct 2013-Febr.14. The data points have been corrected for the dip function and the linear function, optimised in a regression analysis. The horizontal lines indicate the value for the reactor status parameter.

Figure 6 shows the data after being corrected for the dip function and the linear function and showing the reactor status effect. In the analysis the transition periods T , in which the antineutrino flux is changing due to the fuel cooling or the ramp-up of the reactor, have been omitted.

Table 2. Resulting $\Delta A/A$ values for three RoI, during two measurement series and their average values. For the weighted averages the systematic uncertainty reflecting the uncertainty in the ON/OFF BG ratio has been given in italics.

	$\left[\frac{\Delta A}{A}\right]_{TOT} * 10^4$	$\left[\frac{\Delta A}{A}\right]_{MED} * 10^4$	$\left[\frac{\Delta A}{A}\right]_{HI} * 10^4$
Febr.-May 2013	-3.2 ± 0.2	$+1.3 \pm 0.7$	-3.3 ± 0.4
Oct.-Febr. 2014	-3.1 ± 0.2	$+0.7 \pm 0.7$	-2.8 ± 0.4
Weighted Average	$-3.11 \pm 0.15 \pm 0.08$	$+1.02 \pm 0.45 \pm 0.11$	$-3.04 \pm 0.26 \pm 0.03$

The data show that the (ON-OFF)/OFF effect ($\Delta A/A$) on the count rate in the two measurement periods are highly similar or in other words the effect is reproducible. This also stands out from the values listed in Table 2. From the table one also notices that the systematic uncertainties due to the statistical uncertainties in the BG ON/OFF ratios is small compared to the statistical uncertainty resulting from the regression analysis. The importance of the systematic uncertainties decreases with increasing RoI energy, which

reflects the more or less exponential shape of the continuum in the background (see e.g. Figure 3) and the almost linear continuum in the ^{22}Na spectrum.

Implications.

The results in Table 2 indicate that the $\Delta A/A$ effect in ^{22}Na are an order of magnitude larger than in ^{60}Co . This is consistent with a physics related cause for the $\Delta A/A$ effect in ^{22}Na . The negative sign of the effect indicates that the effect is not due to an additional reaction, which would have caused an increase in count rate during ON compared to OFF. Hence the most likely physics effect is an effect of antineutrinos on the β^+ -decay, reducing its branching ratio and thereby reducing the decay constant of ^{22}Na .

If the observed effect on the ^{22}Na are due to physics the results should comply with a consistency check on the decay properties of ^{22}Na . From the basic decay law:

$A = \lambda N$, where λ is the decay constant and N the number of nuclei, it follows that

$$\frac{\Delta A}{A} = \frac{\Delta \lambda}{\lambda}$$

And hence the fractional ratios $R = \frac{\Delta A}{A}$ contain information on partial decay constants, λ_i , and corresponding branching ratio for decay mode i : $BR(i) = \lambda_i / \lambda$. Since the ground-state transition is very weak we limit the check to EC and β^+ -decay to the $^{22}\text{Ne}(1)$ state at $E_x = 1.275$ MeV with $\lambda = \lambda_{EC} + \lambda_{\beta^+}$.

As noticed RoI HI is due to β^+ -decay solely and in addition is rather insensitive to systematic errors due to uncertainties in the background. So we obtain $R_{HI} = \Delta \lambda_{\beta^+} / \lambda_{\beta^+}$. We assume that the reactor status has no effect on EC. In that case $\Delta \lambda = \Delta \lambda_{\beta^+}$ and $\frac{R_{TOT}}{R_{HI}} =$

$$\frac{\Delta \lambda}{\lambda} * \frac{\lambda_{\beta^+}}{\Delta \lambda_{\beta^+}} = \frac{\lambda_{\beta^+}}{\lambda} = BR(\beta^+).$$

From Table 2 we find $BR(\beta^+) = 1.02 \pm 0.10$ with only statistical uncertainties. The measured value is 0.9033.

Next we question the meaning of the positive value for R_{MED} . If RoI MED would only contain EC events then since $\Delta BR(EC) = -\Delta BR(\beta^+)$ the expected value for $R_{MED} = \Delta \lambda_{EC} / \lambda_{EC} = 3.04 * 10^{-4} / 0.092 = 33 * 10^{-4}$. The measured value of $(1.0 \pm 0.5) * 10^{-4}$ This value is obtained from $33 * 10^{-4} * Br(EC) + (1 - Br(EC)) * -3.04 * 10^{-4} = (1.0 \pm 0.5) * 10^{-4}$. Solving this equation leads to $Br(EC) = 11 \pm 6\%$ compared to $0.0962 / 0.9033 = 11\%$ according to the decay scheme. This is a good agreement.

From these results one may conclude that the properties of the observed reactor-status effect on the count rate of ^{22}Na are consistent with the expectations based on the decay properties of ^{22}Na . This implies that these results indicate that nuclear decay can be influenced by outside factors, which is in contradiction with the general consensus.



Another unexpected result is the cross section for this antineutrino based effect. The change in count rate relative to the reactor-OFF count rate: $\Delta A_{ON-OFF} / A_{OFF}$ is directly related to the change in decay constant, λ , and the associated cross section, σ , for the process leading to the change: $\sigma = \frac{|\Delta\lambda|}{\Delta\phi_\nu} = \frac{\lambda}{\Delta\phi_\nu} \frac{|\Delta\lambda|}{\lambda}$

where $\Delta\phi_\nu$ is the difference in antineutrino flux between Reactor=ON and Reactor=OFF, under the assumption that all effects are due to antineutrino interactions only.

The decay constants for ^{22}Na and ^{60}Co are $8.442 \cdot 10^{-9}$ and $4.167 \cdot 10^{-9} \text{ s}^{-1}$ based on the half-lives listed in *Tables of Isotopes*. With fractional count rates of $\Delta A_{ON-OFF} / A_{OFF}$ of $(-3.0 \pm 0.5) \cdot 10^{-4}$ and $(-0.2 \pm 0.6) \cdot 10^{-4}$ and a change in antineutrino flux of $\Delta\phi_\nu = 1.48 \cdot 10^{13} \text{ cm}^{-2}\text{s}^{-1}$ the corresponding cross sections become $(1.8 \pm 0.2) \cdot 10^{-25}$ and $(0.1 \pm 0.2) \cdot 10^{-25} \text{ cm}^2$ for ^{22}Na and ^{60}Co and statistical uncertainties only, respectively. As mentioned above the value for ^{60}Co is consistent with zero and reflects a detection limit. For ^{22}Na the value exceeds the well-known value of 10^{-43} cm^2 for antineutrino capture by a free proton by 18 orders of magnitude.

2.1.5. Fermi's Golden Rule

In a simplified way we like to clarify the difference between the wave functions for the initial and final states in the ^{22}Na case.

According to Fermi's Golden Rule the decay constant, λ is given as:

$$\lambda = \frac{2\pi}{\hbar} |M_{if}|^2 * \rho_{PS},$$

where ρ_{PS} stands for the density of states (Phase Space) The Matrix element M_{if} is defined as:

$$|M_{if}|^2 = \langle \Psi_i | H_{if} | \Psi_f \rangle.$$

In our case the operator H_{if} stands for the Gamov-Teller operator.

For the β^+ -decay of ^{22}Na and reactor=OFF the initial and final wave functions are given by:

$$\Psi_i = \Psi_{^{22}\text{Na}(0)} \text{ and } \Psi_f = \Psi_{^{22}\text{Ne}(1)} \varphi_{e^+} \Psi_{\nu_e},$$

and

$$|M_{if}|^2 = \langle \Psi_{^{22}\text{Na}(0)} | H_{if} | \Psi_{^{22}\text{Ne}(1)} \varphi_{e^+} \Psi_{\nu_e} \rangle,$$

which leads to λ_{OFF} .

For reactor=ON the source decays in a flux of antineutrinos and we write:

$$\Psi_i = \Psi_{^{22}\text{Na}(0)} \Psi_{\bar{\nu}_e} \text{ and } \Psi_f = \Psi_{^{22}\text{Ne}(1)} \varphi_{e^+} \Psi_{\nu_e} \Psi_{\bar{\nu}_e},$$

Note that in the outgoing channel the wave functions of neutrino and antineutrino show up. If these two antiparticles would have a final-state interaction and subsequently annihilate the matrix element would become:

$$|M_{if}|^2 = \langle \Psi_{^{22}\text{Na}(0)} \Psi_{\bar{\nu}_e} | H_{if} | \Psi_{^{22}\text{Ne}(1)} \varphi_{e^+} \rangle * \langle \Psi_{\nu_e} | H_{fs} | \Psi_{\bar{\nu}_e} \rangle,$$

where H_{fs} is the operator for the final-state interaction. This equation leads to λ_{ON} .



2.1.6. Conclusions

Although we are suspiciously surprised by the 18 orders of magnitude larger cross section for the reactor status effect in ^{22}Na compared to the free proton, and having carefully investigated possible systematic effects we have found that:

- the effect is reproducible with consistent values with the uncertainties;
- the effect is more than five times the uncertainty (5 sigma criterion);
- the size and sign of the effect for various RoI in the energy spectrum are consistent with the branching ratios and an effect only affecting β^+ -decay (internal consistency).
- for β^+ -decay the negative sign of the effect excludes contributions from capture reactions.
- the effect on β^- -emitter ^{60}Co is an order of magnitude smaller than for ^{22}Na and the uncertainty in the experiment (check on instrumental and/or procedural causes).
- There is no-effect of a antineutrino capture on ^{50}V (check on instrumental and/or procedural causes).

Based on these finding we have to conclude that the $\Delta A/A$ effect in ^{22}Na is real and has a physics cause. The negative sign indicates that there is a yet unknown process in which the antineutrinos are involved. The huge difference in the cross section between this process and the antineutrino capture on a free proton is suggestive for the formation of a resonance/pseudo particle at very low antineutrino energies such as an neutrino-antineutrino pair similar to positronium.

2.1.7 Outlook

The next step in the development of an antineutrino monitor of nuclear installations from some distance we plan to use the outage of Unit#1 at Koeberg to install a stronger source and updated hard- and software. With a 50kBq source we have a 25 times higher count rate and are in principle 5 times more sensitive. It would mean, that if background is no problem such a detector system could be placed at about 80m from the core and have the same sensitivity as the present set up. If this step (Koeberg-05) is made successfully, a 1m^3 detector system encompassing nine detectors is foreseen that may be placed at a quarter of a kilometre from the core. This will be the proto-type of REACTOR CAM-01 as indicated in Figure 1.

In parallel we continue to use the present set up to locate sources that have per Bq a larger $\Delta A/A$ effect than ^{22}Na and will try to understand the mechanism leading to the effect. If successful this may lead an increase in sensitivity and thereby may open the way to surveillance by drones for non-proliferation violations and/or the building of detector systems for geoscience and technology applications.



Potential applications for routine safeguards and nuclear non-proliferation and verification

The deployment and routine use of antineutrino detection systems in support of nuclear safeguards at reactor sites will provide national, regional and international nuclear verification organizations with the ability to monitor a reactor's power (ON/OFF) status, its relative operating power level and, potentially, its core burn-up ratio of uranium to plutonium. A complete system will be a stand-alone instrument, contained securely and entirely within a sealable, tamper indicating enclosure, offering internal data recording for subsequent pick-up and review. Additionally, the instrument will be able to transmit its data securely to a remote field, regional or international safeguards office for timelier reactor operation verification. Due to the fact that antineutrinos cannot be shielded, the self-contained detection system can be located outside the reactor's biological barrier, and perhaps even away from the reactor's containment building, facilitating inspector and maintenance access. Unlike other neutron and gamma based instruments, the compact antineutrino system will require only connections to facility electrical mains and an optional connection to a data line (telephone, ADSL, satellite, etc.), thus eliminating in-facility cabling, while simplifying installation and reducing deployment costs. All these items are part of the International Atomic Energy Agency (IAEA) Novel Technologies Project and have been defined by its Working Group on Safeguards Applications utilizing Antineutrino Detection and Monitoring, (*IAEA Report SG-EQ-GNRL-RP-0002, 2012*).

Tools that are capable of detecting undeclared nuclear materials, activities and facilities are crucial to non-proliferation implementation. With the present development of the EARTH antineutrino detector systems (e.g. REACTOR CAM-01) becoming increasingly more feasible additional studies should be undertaken to assess the technique in support of non-proliferation applications. The relative small size of the EARTH antineutrino detection package will enable the development of transportable systems, for vehicular use on the ground and Airborne detection systems. Since flying above the ground beyond 100 metres hardly requires gamma shielding, the EARTH detector systems are also envisaged for both manned and unmanned aerial vehicle (UAV) payloads. Such systems would be suitable for the detection of undeclared above, or underground, activities or operating facilities.

Of course the above applications for both routine safeguards and non-proliferation applications are based on extrapolations from the present results (such as ON/OFF status, its relative operational level and changes in the burn-up ratio of U and Pu), and the assumption that the basic mechanisms of the physics behind the effects are fully understood. At the appropriate time, and with sufficient funding, each will require a full assessment and successful demonstration as a practical and effective tool in support of its intended function.



2.1.8 Acknowledgements

This work is financially supported in part by the Dutch Ministry of Foreign Affairs as part of the Member State Support Programme (MSSP) of IAEA, the Department of Physics University of the Western Cape and donations (in money and in kind) made to Stichting (Foundation) EARTH. The authors are very thankful to the Koeberg Nuclear Power Station for providing us access to the facility.



3 Neutrino Geoscience.

3.1. Introduction.

The long-term scientific goal of the EARTH Foundation is to work towards obtaining a 3D-image of the distribution of radiogenic heat sources in the interior of the Earth by means of antineutrino tomography. Although in the short term the present detector development focuses on reactor monitoring, this long-term goal remains unchanged. On the basis of the rapidly growing geoscience literature on these topics and in the absence of any data, we are exploring the nature of the radiogenic heat sources being either natural radioactive decay, or possibly a natural georeactor. In both cases antineutrinos will be emitted, but a distinction between the two types can be made from their energy spectrum. As indicated in earlier work (*de Meijer and van Westrenen, 2008*) our present knowledge of geoscience cannot rule out georeactors in the core-mantle boundary (CMB) region in the Earth, at depths of approximately 2900 km.

In the previous progress report (EARTH-PRP-10) we described the nuclear explosion model for the formation of the Moon that we developed in a collaboration with with dr V. F. Anisichkin of the Lavrentyev Institute of Hydrodynamics, Siberian Branch of Russian Academy of Sciences, Novosibirsk, Russia. In a joint paper, finally published in *Chemical Geology*, we re-examined the dynamics of the Earth-Moon system and the energetics of initial Earth-Moon separation. In contrast to previous ‘fission’ models, our conservative assumption is that the angular momentum of the proto-Earth before Moon formation is close to that of the present-day Earth-Moon system. This is in full agreement impact origin for the Moon (*Canup, 2008*). We estimate the amount of energy required to separate the Moon from the Earth in this case and propose nuclear fission as the only known natural process that could supply the missing energy in such a very short time (*de Meijer et al., 2013*

As a next step we have examined various stability-related boundary conditions imposed by a proto-Earth and a Earth-Moon system to comply with basic physics. This work was carried out in a collaboration between the Geoscience Department of the University of Utrecht (dr. Inge Loes ten Kate and BSc student Maarten Reuver) and the VU University Amsterdam - Faculty of Earth and Life Sciences.

Our present calculations (*Reuver et al., 2016*) indicate that the proto-Earth in the calculations of Čuk and Stewart (2013) is not dynamically stable and would break-up even before a collision. In the calculations of Canup (2012) the post-collision Earth is rotating too fast for dynamic stability and produces a second moon.

4. References.

Canup, R.M., 2008. Lunar forming collisions with pre-impact rotation. *Icarus* **196**, 518-538.

Canup, R.M., 2012. Forming a Moon with an Earth-like composition via a giant impact. *Science* **338**, 1052-1055.

Čuk, M. Stewart, S.T., 2012. Making the Moon from a fast-spinning Earth: A giant impact followed by resonant despinning. *Science* **338**, 1047-1052.

Firestone, R.B., et al, 1996, Table of Isotopes, 8th edition, John Wiley and Sons, New York.

IAEA Report for General Distribution, *Proceedings of the first meeting of the Ad Hoc Working Group on Safeguards Applications utilizing Antineutrino Detection and Monitoring*, 29 August 2012, Vienna SG-EQ-GNRL-RP-0002.

de Meijer, R.J., Anisichkin, V.F., van Westrenen, W., 2013. Forming a Moon from terrestrial silicate-rich material. *Chemical Geology* **345**, 40-49.

de Meijer, R.J. and van Westrenen, W., 2008. The feasibility and implications of nuclear georeactors in Earth's core-mantle boundary region, *South African Journal of Science*, **104**, 111-118.

de Meijer, R.J., Blaauw, M, and Smit, F.D., 2011. No evidence for antineutrinos significantly influencing exponential β^+ decay, *Applied Radiation and Isotopes*, **69**, 320-326. [doi:10.1016/j.apradiso.2010.08.002](https://doi.org/10.1016/j.apradiso.2010.08.002)..

de Meijer, R.J. and Steyn, S.W., Upper limit on the cross section for reactor antineutrinos changing ²²Na decay rates, 2014 ArXiv.org: 1409.6969.

Reuver, M., de Meijer, R.J., ten Kate, I.L. , van Westrenen, W., 2016, Boundary conditions for Moon formation, *Netherlands Journal of Geosciences*, **95**, 131-139.

